Spectrochimica Acta Part A: Molecular and Biomolecular Spectroscopy 129 (2014) 421–428

Contents lists available at ScienceDirect

Spectrochimica Acta Part A: Molecular and Biomolecular Spectroscopy

journal homepage: www.elsevier.com/locate/saa

Ab initio/DFT calculations of tert-butyl ammonium salt of O,O′-dibornyl dithiophosphate

H.H. Kart [a,*], S. Özdemir Kart [a], M. Karakuş [b], M. Kurt [c]

[a] Department of Physics, Pamukkale University, Kinikli, 20017 Denizli, Turkey
[b] Department of Chemistry, Pamukkale University, Kinikli, 20017 Denizli, Turkey
[c] Department of Physics, Ahi Evran University, 40100 Kırşehir, Turkey

HIGHLIGHTS

- O,O′-dibornyl dithiophosphete has been synthesized.
- The compound has been characterized by IR, ^{1}H and ^{13}C NMR spectroscopy.
- DFT/B3LYP results are more compatible with the measured results.

GRAPHICAL ABSTRACT

O,O′-dibornyl dithiophosphate has been synthesized by the reaction of P_2S_5 and borneol in toluene.

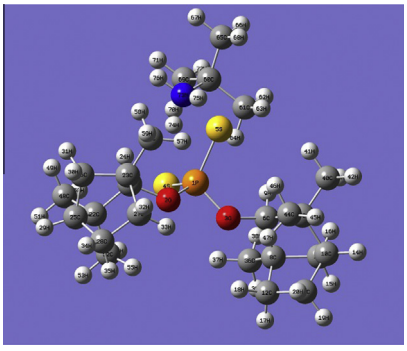

ARTICLE INFO

Article history:
Received 7 January 2014
Received in revised form 5 March 2014
Accepted 23 March 2014
Available online 2 April 2014

Keywords:
FT-IR
NMR
DFT and HF
Dithiophosphate

ABSTRACT

O,O′-dibornyl dithiophosphate has been synthesized by the reaction of P_2S_5 and borneol in toluene. Fourier Transform Infrared spectra (FT-IR) of the title compound are measured. The molecular geometry, vibrational frequencies, infrared intensities and NMR spectrum of the title compound in the ground state have been calculated by using the density functional theory (DFT) and ab initio Hartree–Fock (HF) methods with the basis set of 6-31G(d). The computed bond lengths and bond angles show the good agreement with the experimental data. Moreover, the vibrational frequencies are calculated and the scaled values have been compared with experimental FT-IR spectra. Assignments of the vibrational modes are made on the basis of total energy distribution (TED) calculated with scaled quantum mechanical (SQM) method. The observed and calculated FT-IR and NMR spectra are in good agreement with each other.

Introduction

Dithiophosphates compounds $[(RO)_2P(S)SH]$ and their metal complexes are an important class in organophosphorous chemistry [1–5] due to utilizing in agricultural, medicinal and technological fields [6,7]. Dithiophosphates or O,O′-dialkyldithiophosphoric acids can be synthesized by the reaction of P_2S_5, which is commercially available reagent, and the corresponding alcohols. Therefore, there are many dithiophosphates in the previous reports and some of their properties have been investigated. For example, zinc-dialkyl dithiophosphate complexes (ZDDP) have been known antiwear

* Corresponding author. Tel.: +90 2582963588; fax: +90 2582963535.
E-mail address: hkart@pau.edu.tr (H.H. Kart).

http://dx.doi.org/10.1016/j.saa.2014.03.076
1386-1425/

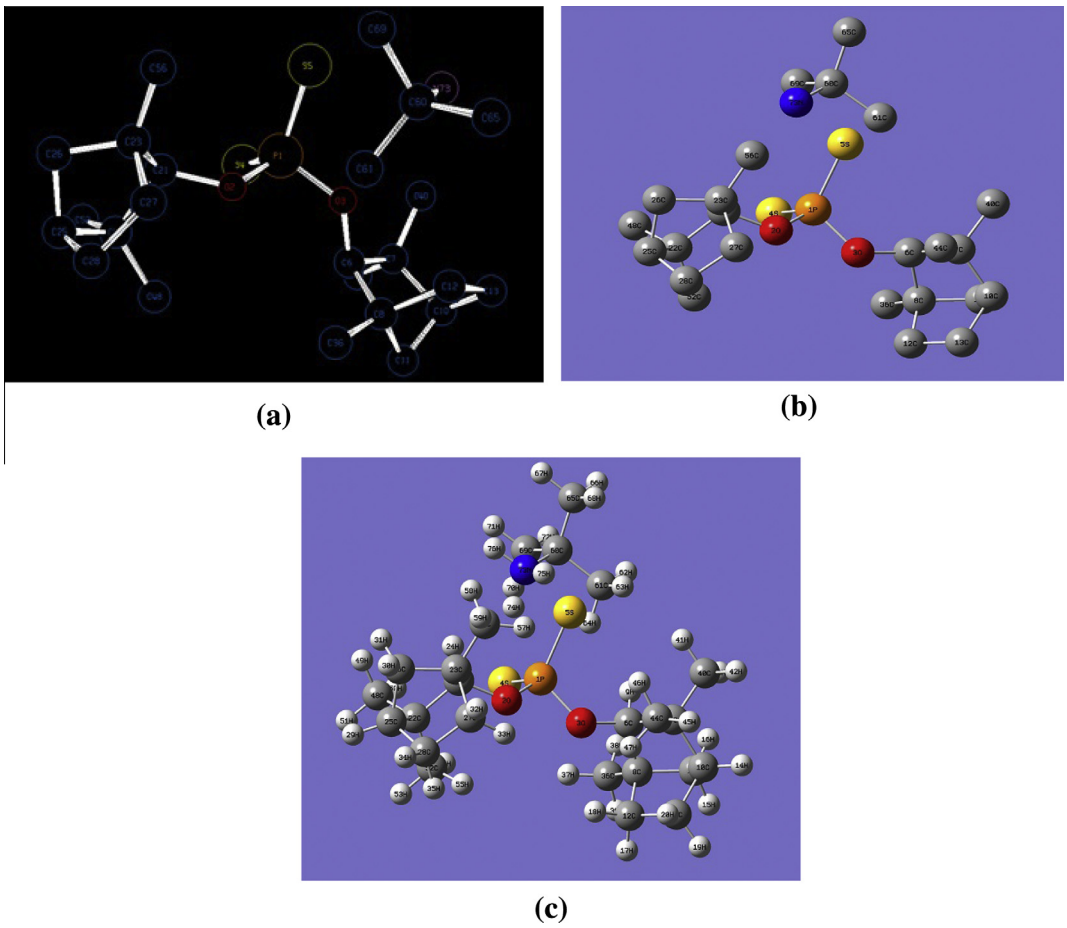

Fig. 1. (a) Experimental molecular structure of the title compound with the atom-numbering scheme. Hydrogen bonds are not shown to clarify the structure of the compound as dashed lines. (b) The optimized theoretical geometric structure of the title compound with the atomic numbering scheme without hydrogen atoms. (c) The optimized geometric structure of the title compound shows all the atoms with the atomic labeling of the atoms.

additive in engine oil [6]. So and Lin have investigated the properties of ZDDP, such as the effects of temperature, the effects of surface roughness and they have clarified the performance of ZDDP in the boundary lubrication medium [6].

In our previous study [7], phosphorus-1,1-dithiolate ligands have been synthesized and then utilized in the preparation of gold(I) and silver(I) phosphorus 1,1-dithiolates. Both of the experimental studies and theoretical calculations on the structural and vibrational properties of the title compound are scarce in the literature. In order to comprehend and understand the experimental studies and to provide insight into molecular parameters and vibrational spectra, theoretical studies need to be performed to characterize the fundamental properties of the title compound.

The theoretical studies provide important information about the physical and chemical properties of the compounds. For example, vibrational spectroscopy is a versatile and readily available tool for interpreting and predicting the properties of chemically and biologically active molecules. It has been used both in the study of chemical kinetics and chemical analysis. However, the assignment of band as well as the understanding of the relationship between the observed spectral features and the molecular structure can be difficult [8]. Ab initio methods such as Hartree–Fock (HF) and Density Functional Theory (DFT) in the computational chemistry are important tools to predict the structural properties of the molecules and to determine their vibrational spectra. Ab initio calculations based on the quantum mechanics are widely used to study some physical and chemical properties of the materials and chemical compounds [9,10]. Recently, DFT and HF methods are widely used to determine the molecular structures and vibrational spectra for small and large sized chemical molecules at low computational cost [11–30]. These computational methods used in computational chemistry generally give rise to systematic errors mainly due to the limited basis sets, the harmonic approximation and the remaining deficiencies in describing electron correlation [31]. In order to overcome these errors, some theoretical methods have been used for fitting of the calculated vibrational frequencies to experimentally observed ones.

The studies on chemical shift calculations based on quantum chemistry methods show that the geometry optimization of the molecule is an important factor to determine the NMR chemical shifts accurately [32].

To the best of our knowledge, the quantum chemical computations of the title compound have not been carried out up to now. Therefore, in the present work, we have compared the experimental to theoretical results of the title compound by using the ab initio calculations methods based on DFT and HF levels. A comparison of the experimental and theoretical calculations can be very useful for making a correct assignment and understanding the basic vibrational, NMR spectra and molecular structure relations. In other words, a discussion on the experimental and theoretical studies of this compound leads to a better understanding of the nature of the title compound.

Table 1
The optimized and experimental geometrical parameters of title compound in the ground state. The experimental data are taken from our previous study [7].

	Bond labels via Gaussian (Å)	Bond length (Å) from experimental crystal	Experimental	DFT/B3LYP/6-31G(d)	HF/6-31G(d)
1	R(1,2)	P1–O2	1.610(11)	1.628	1.589
2	R(1,3)	P1–O3	1.591(11)	1.627	1.589
3	R(1,4)	P1–S4	1.976(5)	2.026	2.006
4	R(1,5)	P1–S5	1.981(5)	2.027	2.005
5	R(2,21)	O2–C21	1.449(18)	1.442	1.422
6	R(3,6)	O3–C6	1.450(17)	1.442	1.422
9	R(6,7)	C6–C7	1.572(2)	1.583	1.572
10	R(6,8)	C6–C8	1.533(2)	1.553	1.543
12	R(7,10)	C7–C10	1.549(2)	1.565	1.556
13	R(7,40)	C7–C40	1.531(2)	1.542	1.538
14	R(7,44)	C7–C44	1.531(2)	1.536	1.533
15	R(8,11)	C8–C11	1.540(2)	1.547	1.538
16	R(8,12)	C8–C12	1.548(2)	1.555	1.547
17	R(8,36)	C8–C36	1.510(2)	1.522	1.520
18	R(10,11)	C10–C11	1.538(2)	1.544	1.537
19	R(10,13)	C10–C13	1.537(2)	1.545	1.538
23	R(12,13)	C12–C13	1.548(3)	1.560	1.553
31	R(22,25)	C22–C25	1.532(3)	1.565	1.556
32	R(22,48)	C22–C48	1.515(3)	1.542	1.538
33	R(22,52)	C22–C52	1.560(3)	1.536	1.533
37	R(25,26)	C25–C26	1.517(3)	1.543	1.537
38	R(25,28)	C25–C28	1.555(3)	1.545	1.538
65	R(60,61)	C60–C61	1.518(2)	1.534	1.529
66	R(60,65)	C60–C65	1.524(3)	1.534	1.528
67	R(60,69)	C60–C69	1.528(3)	1.534	1.528
68	R(60,73)	C60–N73	1.501(2)	1.513	1.503
	Bond angles (°) from Gaussian	Bond angles (°) from experimental crystal	Experimental	DFT/B3LYP/6-31G(d)	HF/6-31G(d)
1	A(2,1,3)	O2–P1–O3	99.61(6)	93.18	95.99
2	A(2,1,4)	O2–P1–S4	110.12(4)	111.28	110.93
3	A(2,1,5)	O2–P1–S5	110.05(4)	111.37	110.92
4	A(3,1,4)	O3–P1–S4	113.30(4)	111.40	110.95
5	A(3,1,5)	O3–P1–S5	105.02(4)	111.43	110.98
6	A(4,1,5)	S4–P1–S5	117.23(2)	115.96	115.42
7	A(1,2,21)	P1–O2–C21	121.47(9)	123.94	128.68
8	A(1,3,6)	P1–O3–C6	124.65(9)	124.13	128.66
11	A(3,6,7)	O3–C6–C7	113.38(12)	112.99	113.01
12	A(3,6,8)	O3–C6–C8	110.06(11)	110.98	111.04
14	A(7,6,8)	C7–C6–C8	104.89(12)	104.90	104.77
17	A(6,7,10)	C6–C7–C10	101.24(12)	101.02	101.17
18	A(6,7,40)	C6–C7–C40	113.14(13)	110.38	110.73
19	A(6,7,44)	C6–C7–C44	110.29(14)	113.32	113.40
20	A(10,7,40)	C10–C7–C40	114.01(14)	110.16	109.95
21	A(10,7,44)	C10–C7–C44	109.41(14)	114.06	114.06
22	A(40,7,44)	C40–C7–C44	108.57(15)	107.81	107.48
23	A(6,8,11)	C6–C8–C11	99.11(12)	99.52	99.59
24	A(6,8,12)	C6–C8–C12	107.87(13)	108.21	108.73
25	A(6,8,36)	C6–C8–C36	114.03(14)	114.51	114.40
26	A(11,8,12)	C11–C8–C12	101.52(13)	101.09	101.07
27	A(11,8,36)	C11–C8–C36	117.07(13)	117.16	117.04
28	A(12,8,36)	C12–C8–C36	115.34(14)	114.54	114.29
32	A(11,10,13)	C11–C10–C13	100.01(14)	100.22	100.02
35	A(8,11,10)	C8–C11–C10	95.05(12)	95.22	95.05
41	A(8,12,13)	C8–C12–C13	104.15(13)	103.96	103.87
47	A(10,13,12)	C10–C13–C12	102.62(14)	102.85	102.79
53	A(2,21,22)	O2–C21–C22	112.75(12)	113.31	112.98
54	A(2,21,23)	O2–C21–C23	111.97(13)	110.64	111.05
56	A(22,21,23)	C22–C21–C23	104.53(13)	104.86	104.79
59	A(21,22,25)	C21–C22–C25	102.30(14)	101.01	101.17
60	A(21,22,48)	C21–C22–C48	113.92(14)	110.33	110.72
61	A(21,22,52)	C21–C22–C52	109.38(15)	113.49	113.40
62	A(25,22,48)	C25–C22–C48	115.68(17)	110.17	109.96
63	A(25,22,52)	C25–C22–C52	109.09(15)	113.91	114.07
64	A(48,22,52)	C48–C22–C52	106.35(17)	107.83	107.48
65	A(21,23,26)	C21–C23–C26	99.17(14)	99.57	99.57
66	A(21,23,27)	C21–C23–C27	107.05(16)	108.18	108.73
67	A(21,23,56)	C21–C23–C56	116.06(18)	114.41	114.40
68	A(26,23,27)	C26–C23–C27	99.67(19)	101.07	101.07
69	A(26,23,56)	C26–C23–C56	118.95(19)	117.31	117.05
70	A(27,23,56)	C27–C23–C56	113.7(2)	114.50	114.30
71	A(22,25,26)	C22–C25–C26	102.95(16)	102.27	102.20
72	A(22,25,28)	C22–C25–C28	109.21(16)	111.08	111.30
74	A(26,25,28)	C26–C25–C28	98.48(18)	100.25	100.02
77	A(23,26,25)	C23–C26–C25	97.34(16)	95.19	95.05

(*continued on next page*)

Table 1 (*continued*)

	Bond labels via Gaussian (Å)	Bond length (Å) from experimental crystal	Experimental	DFT/B3LYP/6-31G(d)	HF/6-31G(d)
83	A(23,27,28)	C23–C27–C28	104.18(17)	103.99	103.88
89	A(25,28,27)	C25–C28–C27	103.19(18)	102.82	102.79
131	A(61,60,65)	C61–C60–C65	112.01(18)	111.42	111.48
132	A(61,60,69)	C61–C60–C69	111.69(16)	111.45	111.47
133	A(61,60,73)	C61–C60–N73	107.47(14)	107.11	107.26
134	A(65,60,69)	C65–C60–C69	111.72(17)	111.53	111.64
135	A(65,60,73)	C65–C60–N73	107.73(15)	107.52	107.36
136	A(69,60,73)	C69–C60–N73	105.86(15)	107.55	107.34
	Dihedral angles (°) from Gaussian	Dihedral angles (°) from experimental crystal	Experimental	DFT/B3LYP/6-31G(d)	HF/6-31G(d)
1	D(3,1,2,21)	O3–P1–O2–C21		−173.41	−154.89
2	D(4,1,2,21)	S4–P1–O2–C21		−58.96	−39.73
3	D(5,1,2,21)	S5–P1–O2–C21		72.10	89.93
4	D(2,1,3,6)	O2–P1–O3–C6		−168.67	−155.35
5	D(4,1,3,6)	S4–P1–O3–C6		76.98	89.51
6	D(5,1,3,6)	S5–P1–O3–C6		−54.22	−40.22
7	D(2,1,4,74)	O2–P1–S4–H74		126.69	125.53
8	D(3,1,4,74)	O3–P1–S4–H74		−130.80	−129.03
9	D(5,1,4,74)	S5–P1–S4–H74		−1.96	−1.70
10	D(2,1,5,75)	O2–P1–S5–H75		−126.21	−125.60

This paper is organized as follows: materials and equipment are presented in Section 'Experimental details'. The calculation method is introduced and the computational details are given in Section 'Computational details'. The simulation results for structural and vibrational properties of the title compound considered in this study are presented and discussed in Section 'Results and discussion'. We have also compared our results with the available experimental data in Section 'Results and discussion'. Finally, the summary of our main results and the conclusion are given in the last section.

Experimental details

All chemical materials are purchased from commercial sources and used directly without further purification. The preparation method of the O,O′-dibornyl dithiophosphate is explained and the crystal structure and characterization of the sample are clarified in our previous work [7]. The crystal structure of the sample obtained from X-ray measurements is given in Fig. 1(a). In this study, we have measured their vibrational frequencies by using the FT-IR spectroscopy. FT-IR spectrum is recorded by a Perkin–Elmer 2000 FT-IR spectrophotometer (4000–400 cm^{-1}). NMR (^1H, ^{13}C) spectra are recorded on a Broker AVANCE DRX 400 NMR spectrometer in the medium of deuterated chloroform ($CDCl_3$).

Computational details

In recent years, DFT and HF methods have become powerful tools to investigate the molecular structure and vibrational spectra [33]. The DFT/B3LYP is well known method in theoretical studies especially for IR and HF method does not consider the electron correlation therefore it is well known method to calculate geometrical parameters. We have performed quantum mechanical calculations with the Gaussian 09 package by using the DFT/B3LYP/6-31G(d) and HF/6-31G(d) methods [34,35] to provide complete information regarding the structural characteristic and the fundamental vibrational modes of the title compound. Molecular structure is optimized to get the global minima of the compound at the level of ab initio DFT/B3LYP and HF methods with the basis set of 6-31G (d) by considering C_1 symmetry (no symmetry constraint).

The optimized geometric structures of the title compound with the atomic numbering scheme are given in Fig. 1(b) and (c), respectively. We have used the optimized structure to calculate the vibrational spectra of the compound by taking the same basis set and computational methods. We have also used it to predict the ^1H and ^{13}C NMR shielding constants by applying the Gauge-Including Atomic Orbitals (GIAO) GIAO–DFT and GIAO–HF methods [35] in the medium of deuterated chloroform ($CDCl_3$). The calculation of the ^1H chemical shift is achieved by using the integral equation formalism of the polarizable continuum model (IEFPCM). The stability of the optimized geometries is satisfied by obtaining non-negative values of all the calculated wavenumbers. The total energy distribution (TED) is predicted by using the PQS program [36] and then the fundamental vibrational modes are characterized by using their TEDs for the assignments of the experimental bands in detail. TED calculations show the relative contribution of the redundant internal coordinates to each normal vibrational modes of the molecule and thus it allows the description of the character of each mode numerically. The harmonic frequencies obtained from ab initio methods are multiplied by the appropriate scaled factors [37] to compare them with the experimental frequencies. The incomplete incorporation of electron correlation and the use of finite basis set in the ab initio calculations lead to some systematic errors. Therefore, we have used the scaled factors as 0.9614 and 0.8953 for DFT/B3LYP and HF methods [37], respectively, in order to determine the vibrational spectra of the molecule accurately. The values of the some vibrational modes corresponding to the optimized geometry of the title compound by performing ab initio calculations based on DFT and HF methods with the basis set of 6-31G(d) are given in Tables 2, along with the available experimental data.

Results and discussion

Molecular geometry

The crystal structure of the title compound with the atom-numbering scheme is shown in Fig. 1(a) as reported in our previous study [7]. The optimized geometric structures with DFT/B3LYP/6-31G(d) method and the atom numbering schemes of the title compound are represented in Fig. 1(b) without hydrogen atoms and in Fig. 1(c) with hydrogen atoms, respectively. The geometry of the title compound possesses C_1 point group symmetry. This compound consists of 76 atoms and has 222 fundamental vibrational modes.

Structural properties

The optimized structural parameters such as bond length, bond angle and dihedral angle of the title compound determined from

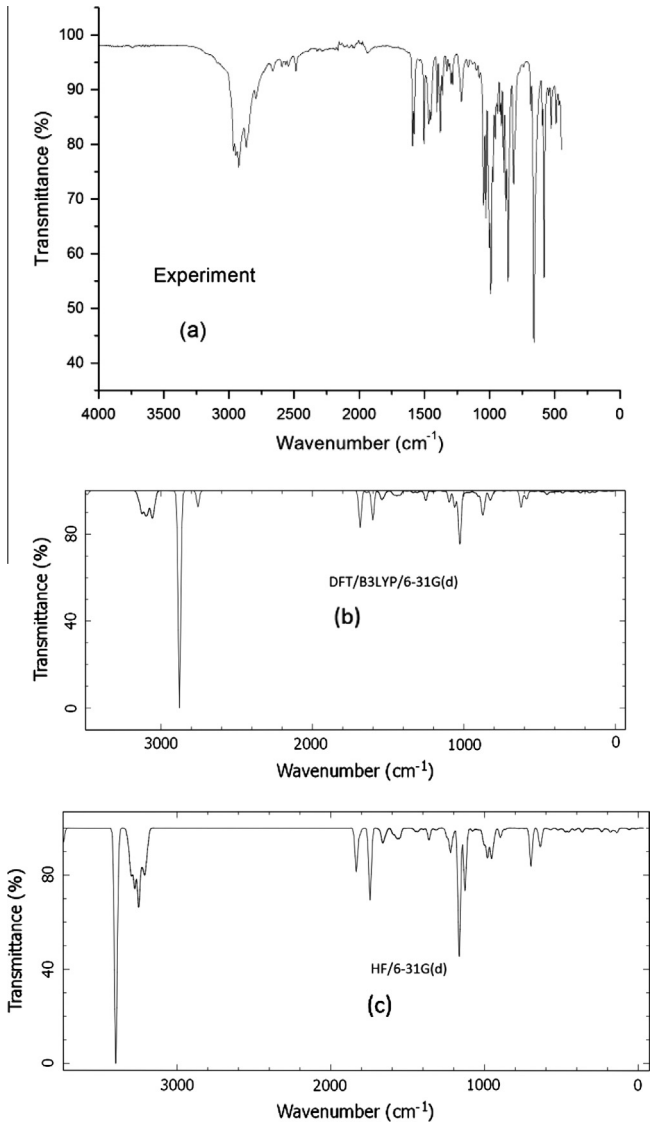

Fig. 2. (a) Experimental, (b and c) the calculated infrared spectra (FT-IR) of the title compound by using DFT/B3LYP and HF methods with the 6-31G(d) basis set, respectively.

DFT/B3LYP and HF levels by using 6-31G(d) as basis set are presented in Table 1. The molecular structure of the title compound consists of 80 bond lengths, 162 bond angles and 260 dihedral angles. These bond lengths, bond angles and dihedral angles given in Table 1 are shown in Fig. 1(b) and (c). We have compared our results of the bond lengths and bond angles with the available corresponding experimental values given in our previous study [7]. As shown in Table 1, they are compatible with each other. The computed bond lengths and bond angles, as shown in Table 1, help us to understand the molecular structure of the title compound. For example, the length of the P1–O2 is measured as 1.610 Å while it is computed as 1.628 Å and 1.589 Å by utilizing the DFT/B3LYP and HF levels with the basis set of 6-31G(d), respectively. The bond angle of the O2–P1–S4 is measured as 110.12° as it is calculated as 111.28° and 110.93° by using DFT and HF methods, respectively. Additionally, 260 dihedral angles of the title compound calculated from DFT/B3LYP and HF levels by using 6-31G(d) as basis set are listed in Table S1 given as a supplementary material. The first 10 dihedral angles for the title molecule are also given at the end of Table 1. The value of the dihedral angle for O2–P1–S4–H74 is computed as 126.69° and 125.53° via DFT and HF levels, respectively. These dihedral angles are not compared with the experimental data which are not available in the literature. But, as shown in Table 1, they are consistent with each other. All the theoretical bond lengths and bond angles characterizing the title compound computed from DFT/B3LYP/6-31G(d) and HF/6-31G(d) are given in Table S1 with the experimental data as a supplementary material.

Analysis of vibrational spectra

Vibrational spectroscopy has been proven to be an important contributor in the study of various fields of science because of the extraordinary versatility of sampling methods. Therefore, it is one of the most useful tools for characterization of the chemical compounds in terms of both experimental studies and theoretical calculations. The investigation of the vibrational frequencies via ab initio computational methods is becoming increasingly important tools in the area of chemistry. Theoretically predicted frequencies can serve ones to determine the fingerprints of the chemical compounds. In the present study, we have performed a frequency calculation analysis to obtain the spectroscopic signature of the title compound. It contains 76 atoms, therefore they have 222 fundamental vibrational normal modes. The experimental FT-IR spectra and theoretical calculations of FT-IR spectra computed from DFT/B3LYP and HF methods by utilizing the basis set of 6-31G(d) of the title compound are plotted in Fig. 2(a), (b) and (c), respectively. Some specific and important vibrational modes calculated by DFT and HF methods are given in Table 2, along with the assignments of fundamental vibration modes. The experimental results are also given in the same table to compare them with

Table 2
Vibrational wavenumbers for the title compound obtained from the B3LYP/6-31G(d) and ab initio HF in cm^{-1}, IR Intensities (km, mol^{-1}), and assignment with TED (obtained from B3LYP/6-31G(d)) percentage in square brackets. Scale factors are taken as 0.9614 and 0.8953 for the DFT/B3LYP/6-31G(d) and HF/6-31G(d), respectively.

Mode No.	B3LYP/6-31G(d)			HF/6-31G(d)			Exp.	
	Unscaled wavenumber	Scaled wavenumber	I^{IR}	Unscaled wavenumber	Scaled wavenumber	I^{IR}	FT-IR	Assignment [TED] ⩾ 10%[a]
56	491.43	472.46	0.75	523.35	468.56	6.60	528	δHSP(19) + δSHN(22)
62	622.53	598.50	159.76	697.55	624.52	195.39	660	νSP(76)
74	878.07	844.18	109.62	954.19	854.29	40.98	991	νOP(37)
75	881.08	847.07	58.03	955.26	855.24	101.97	858	νOP(10)
103	1096.21	1053.90	110.00	1197.20	1071.85	1.28	1047	νCO(61)
174	1601.29	1539.48	288.38	1744.16	1561.55	368.70	1591	δHNC(27) + δHNH(31) + τSHNH(48)
218	3141.13	3019.88	8.10	3317.67	2970.31	34.17	2868	νC(90)
219	3143.67	3022.32	38.64	3318.08	2970.68	20.37	2926	νC(65)
220	3149.75	3028.17	18.26	3388.63	3033.84	223.14	2948	νC(93)
221	3152.71	3031.02	18.09	3399.08	3043.20	1101.41	2965	νC(95)

[a] TED: Total Energy Distribution, ν; stretching, δ; in-plane-bending, γ; out-of plane bending, τ; torsion.

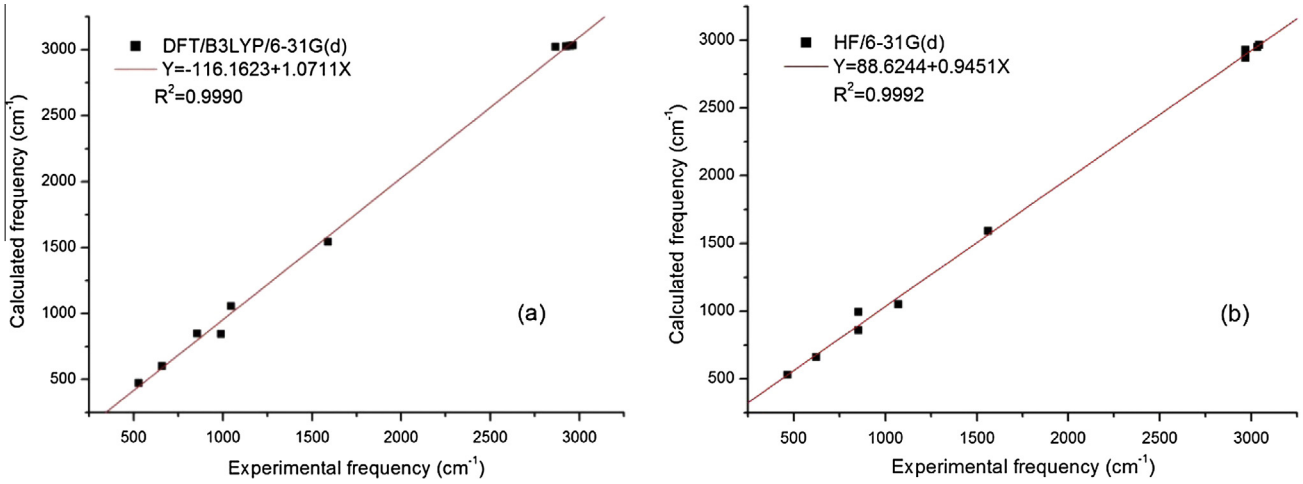

Fig. 3. The correlation graphs between the experimental and calculated wavenumber for the title compound calculated from (a) DFT/B3LYP/6-31G(d) and (b) HF/6-31G(d) levels, respectively.

the corresponding theoretical results. The calculated IR intensities given in the table provide us to distinguish and assign the fundamentals modes more precisely. That is, the calculated infrared intensity (relative intensity) allows determination of the strength of the transition. The infrared intensities predicted at the levels of DFT and HF for the title molecule studied may be followed in Table 2. Note that experimental IR spectra are generally reported in either percent transmission or absorbance unit. Explicitly, this behavior can be seen in Fig. 2. The calculations of vibrational wavenumbers, IR intensity and the assignments of IR vibration modes of all the atoms in the compound are provided in Table S2 as a supplementary material. 222 vibrational modes are shown in Table S2 as well as assignments of them.

The aliphatic C–H stretching vibrations are observed in the region of 2965–2868 cm^{-1} [7]. The scaled aliphatic C–H stretching vibrations at 3031–3020 cm^{-1} and 3043–2970 cm^{-1} are calculated

Table 3
Values of the ^{1}H, ^{13}C NMR chemical shifts (ppm) for the title compound by using the DFT/B3LYP and the HF methods with available experimental data.

Atom	Experimental	DFT/B3LYP		HF		Atom	Experimental	DFT/B3LYP		HF	
	Chloroform	Gas	Chloroform	Gas	Chloroform		Chloroform	Gas	Chloroform	Gas	Chloroform
H74		9.38	9.08	7.86	7.30	H58		0.58	0.71	0.45	0.55
H75		9.31	9.03	7.82	7.28	H38	0.85	0.57	0.72	0.47	0.60
H9	4.64	3.58	3.67	3.07	3.12	H39	0.85	0.55	0.67	0.56	0.61
H24		3.46	3.55	3.04	3.06	H49		0.55	0.74	0.51	0.62
H37	0.85	1.87	1.76	1.91	2.40	H67	0.91	0.54	0.85	0.69	0.93
H18	1.23	1.82	1.77		1.44	H71	0.91	0.53	0.83	0.69	0.93
H57		1.80	1.68	1.87	1.62	H59		0.50	0.64	0.54	0.61
H33		1.77	1.73	1.58	1.43	H42	0.86	0.40	0.51	0.37	0.41
H63	0.91	1.67	1.62	1.60	1.40	H51		0.37	0.49	0.35	0.41
H64	0.91	1.64	1.58	1.66	1.44	H45	0.86	0.22	0.35	0.22	0.29
H41	0.86	1.59	1.54	1.60	1.41	H53		0.20	0.34	0.21	0.29
H20	1.71	1.58	1.62	1.30	1.26	C6	82.50	77.28	77.27	73.68	73.65
H35		1.52	1.59	1.29	1.26	C21		76.84	76.98	73.73	73.75
H50		1.50	1.44	1.58	1.39	C60	53.88	46.5	46.03	43.82	44.49
H29		1.43	1.52	1.10	1.16	C8	49.52	43.46	43.98	39.99	39.97
H14	2.28	1.40	1.49	1.14	1.16	C23		43.46	44.02	39.95	39.91
H54		1.20	1.18	0.99	0.82	C10	47.32	41.61	41.84	39.55	39.35
H34		1.18	1.29	0.91	0.97	C25		41.38	41.60	39.52	39.33
H16	2.00	1.16	1.30	0.82	0.91	C7	37.48	35.49	35.10	32.16	32.08
H19	1.71	1.15	1.27	0.92	0.97	C22		34.91	35.46	32.14	32.08
H68	0.91	1.15	1.16	1.23	1.16	C11	44.93	33.93	34.02	34.60	34.20
H70	0.91	1.13	1.14	1.24	1.17	C26		33.55	33.71	34.58	34.20
H46	0.86	1.12	1.07	1.02	0.83	C27		20.78	21.19	22.14	22.06
H47	0.86	1.12	1.16	1.05	0.99	C12	29.69	20.70	21.17	22.15	22.08
H31		1.11	1.26	0.82	0.90	C13	27.00	20.57	20.93	21.75	21.54
H55		1.09	1.13	1.04	0.99	C48		20.52	21.11	24.53	24.40
H30		0.94	1.06	0.61	0.68	C40	18.57	20.52	21.00	24.57	24.44
H76		0.91	1.86	1.63	2.40	C28		20.50	20.89	21.74	21.53
H15	2.00	0.88	1.00	0.62	0.68	C69	28.31	20.09	20.32	23.98	23.60
H72	0.91	0.83	1.00	0.98	1.07	C65	28.31	20.08	20.34	24.03	23.65
H66	0.91	0.82	1.00	0.98	1.07	C61	28.31	16.16	17.13	21.08	21.49
H32		0.74	0.85	0.61	0.66	C36	13.68	14.37	14.67	19.02	18.66
H17	1.23	0.74	0.84	0.62	0.66	C44	19.94	14.20	14.85	19.06	19.09
H62	0.91	0.65	0.92	0.78	0.99	C52		14.15	14.85	19.08	19.09
H43	0.86	0.59	0.77	0.52	0.63	C56		13.85	14.26	18.85	18.55

by using DFT/B3LYP/6-31G(d) and HF/6-31G(d) methods, respectively. The C–O vibration calculated by performing DFT/B3LYP and HF methods are predicted as 1054 cm^{-1} and 1072 cm^{-1}, respectively, which are compatible with that of experimental data observed at 1047 cm^{-1}. The N–H stretching vibration is exhibited at 1591 cm^{-1} and the theoretical data for N–H stretching vibration is calculated at 1539 and 1562 cm^{-1} by using DFT/B3LYP/6-31G(d) and HF/6-31G(d) methods, respectively. The vibration band at 991 cm^{-1} in FT-IR spectra is assigned to the P–O stretching vibration, which is in agreement with the results computed as 844 cm^{-1} (for DFT) and 854 cm^{-1} (for HF), respectively. The observed bands at 660 cm^{-1} and 528 cm^{-1} are attributed to $\nu_{asym}(PS_2)$ and $\nu_{sym}(PS_2)$, respectively [7]. The corresponding theoretical data are found as 599 cm^{-1}($\nu_{asym}(PS_2)$) and 472 cm^{-1} $\nu_{sym}(PS_2)$ by using DFT method and as 625 cm^{-1} ($\nu_{asym}(PS_2)$) and 469 cm^{-1} $\nu_{sym}(PS_2)$ by using HF method. The other stretching vibrations observed are also given in Tables 2 and S2 as a supplementary. Generally, it is difficult to assign all bands due to the complexity of the stretching vibration bands. In this study, only characteristic stretching vibration bands are identified. Those values are in good agreement with the related study previously reported [1,3].

The correlation graphs of the vibrational frequencies calculated from DFT and HF methods versus their experimental values for the title compound are given in Fig. 3(a) and (b), respectively. The correlation between the experimental and the calculated frequencies which are scaled is linear, as shown in Fig. 3(a) (for DFT) and (b) (for HF). The correlations between the experiment and calculations of DFT and HF methods are described by the equations of $Y = -116.1623 + 1.0711x$($R^2 = 0.9990$) and $y = 88.6244 + 0.9451x$ ($R^2 = 0.9992$, respectively. It can be concluded that the frequency values obtained by the method of HF are more consistent with the experimental data than those obtained by the DFT/B3LYP method, since the slope and the intercept values of the graph obtained by HF calculations goes to unity and zero, respectively, as shown in Fig. 3(b).

NMR spectra

NMR study is an exceptional tool to elucidate structure and conformation of the molecules. Therefore, the characterization of the compound can be further clarified by the use of ^1H and ^{13}C NMR spectroscopy. In other words, NMR shielding contains the detailed information about the electronic structure of the molecules. Thus it provides a sensitive tool to probe the surroundings of nuclei. In addition, GIAO ^1H and ^{13}C chemical shift calculations with respect to Tetramethylsilane (TMS) are carried out by using the DFT/B3LYP and HF with the basis set of 6-31G(d) for the optimized structure in the medium of deuterated chloroform ($CDCl_3$). The results of these calculations are given in Table 3 for the ^1H and ^{13}C chemical shifts in the gas and chloroform media with the available experimental data. The OCH proton of bornyl group gives a triplet at 4.64 ppm in $CDCl_3$. The signals between 2.28 and 1.23 ppm are attributed

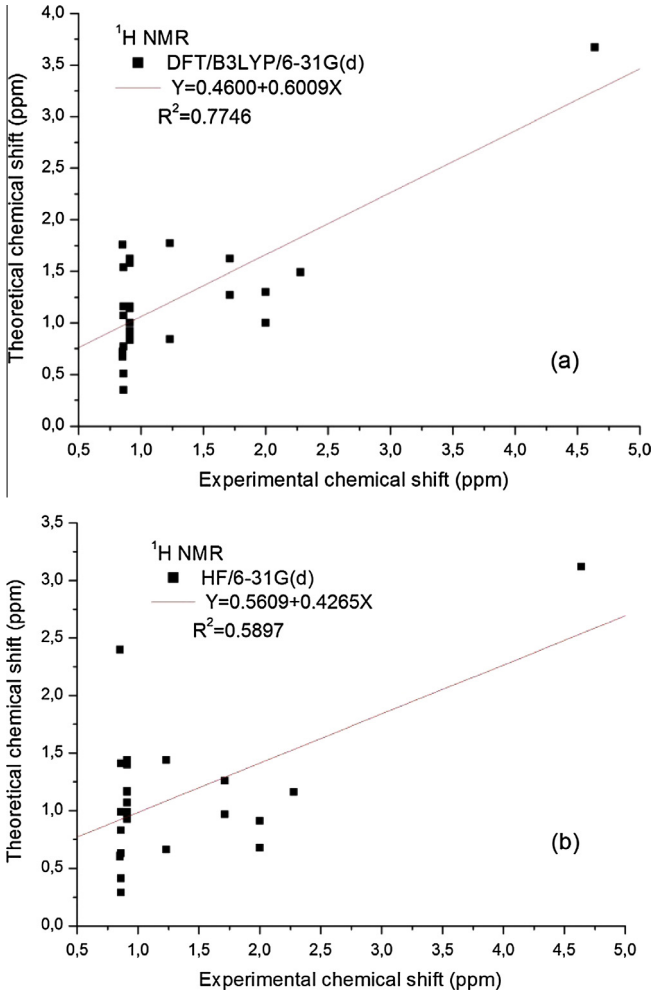

Fig. 4. The correlation graphs between the experimental and theoretical ^1H NMR chemical shift values of the title compound calculated from (a) DFT/B3LYP/6-31G(d) and (b) HF/6–31G(d) levels, respectively.

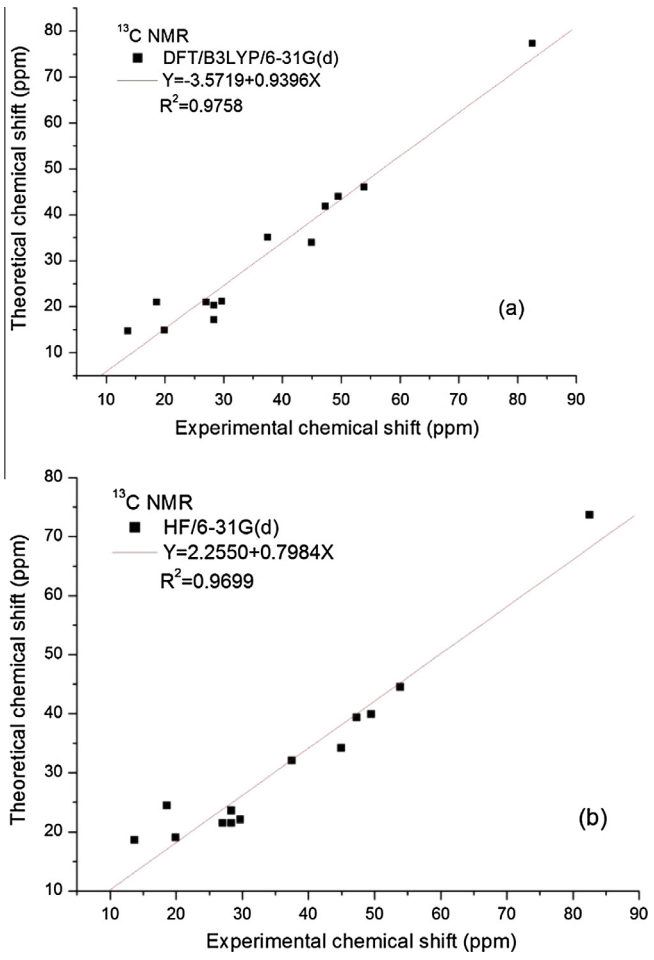

Fig. 5. The correlation graphs between the experimental and theoretical ^{13}C NMR chemical shift values of the title compound calculated from (a) DFT/B3LYP/6-31G(d) and (b) HF/6-31G(d) levels, respectively.

to bornyl ring proton [7]. CH_3 proton of the bornyl ring are observed at 0.85 and 0.86 ppm in $CDCl_3$. It is to say that the values of the NMR computed from DFT and HF methods in the mediums of deuterated chloroform ($CDCl_3$) and gas are compatible with each other. We have investigated the correlations between the calculations computed from DFT/6-31G(d) and experiment to compare them. The linear correlation coefficients (R^2)are obtained by fitting the experimental ^1H and ^{13}C NMR chemical shift values to corresponding values computed by DFT/B3LYP and HF methods, except for the data of 25-H. The results for ^1H and ^{13}C are given in Figs. 4(a), (b) and 5(a) and (b), respectively. As shown in Figs. 4(a) and 5(a), the correlations, ($R^2 = 0.7746$ for ^1H and $R^2 = 0.9758$ for ^{13}C), between the experiment and the calculations obtained by DFT for ^1H and ^{13}C chemical shift in the solvent of $CDCl_3$ are more consistent with those predicted by HF. The correlation ($R^2 = 0.7746$) between the experimental and calculated ^1H chemical shifts for the DFT/B3LYP level is more compatible in the solvent of $CDCl_3$ as shown in Fig. 4(a). The correlation ($R^2 = 0.9758$) between the measured and computed ^{13}C chemical shift for the DFT/B3LYP method is also in good agreement in the solvent of $CDCl_3$ as given in Fig. 5(a). The chemical shift correlations of the ^{13}C by using the DFT/B3LYP and HF methods are closer to the unity than those of ^1H for both methods. DFT and HF methods differ in that electron correlation effects are not taken inco account in HF method while DFT method treat the electronic energy as a function of the electron density of all electrons and thus it includes electron correlation effects. As a result, it can be said that DFT method is superior to compute the chemical shift values of ^1H and ^{13}C for the title compound.

Conclusion

In this paper, DFT and the ab initio HF calculations for the title compound are presented for the first time. Bond lengths, bond angles, dihedral angles, vibrational frequencies and chemical shifts of the title molecule are computed by using DFT and ab initio HF methods. Structural and spectroscopic properties of the title compound are investigated to characterize it. The vibrational analysis is performed for the title compound with the no symmetry, yielding 222 signals being active in IR. The harmonic frequencies calculated from the ab initio methods based on quantum mechanics deviate slightly from the observed frequencies. The one reason of discrepancy between the observed and the calculated frequencies is that the experimental results belong to solid phase while the theoretical calculations have been calculated in the gaseous phase. The another one is that the calculations have been actually performed on a single molecule contrary to the experimental values recorded in the presence of intermolecular interactions. Moreover, the disagreement between the theoretical and the experimental results could be a consequence of the anharmonicity and of the general tendency of the quantum chemical methods to overestimate of the force constants at the exact equilibrium geometry. The correlation equalities for the IR; $Y = -116.1623 + 1.0711x$($R^2 = 0.9990$) and $Y = 88.6244 + 0.9451x$($R^2 = 0.9992$)) are obtained by using the methods of DFT/B3LYP and HF, respectively. Moreover, it can be reported that our DFT calculations produce linear for the chemical shifts behavior, ($R^2 = 0.7746$) in the solvent of $CDCl_3$. Linear regression ($R^2 = 0.7746$) between the experimental and calculated ^1H chemical shifts for the DFT/B3LYP/6-31G(d) level is good in the solvent of $CDCl_3$. Additionally, the correlation ($R^2 = 0.9758$)) between the measured and computed ^{13}C chemical shift by the DFT/B3LYP/6-31G(d) is more compatible than results of HF/6-31G(d), ($R^2 = 0.9699$). It can be concluded that DFT/B3LYP method works well for the prediction of the chemical shift values of ^1H and ^{13}C.

DFT and the ab initio HF methods are valuable and cheap tools for characterizing the chemical compounds.

Acknowledgements

This study has been supported by Pamukkale University and TUBITAK (Grant Nos. 2013FBE009, 2013FBE013). We would like to thank Elif Yeşil for critical reading of this work.

Appendix A. Supplementary material

Supplementary data associated with this article can be found, in the online version, at http://dx.doi.org/10.1016/j.saa.2014.03.076.

References

[1] M.D. Santana, G. Garcia, C.M. Navarro, A.A. Lozano, J. Perez, L. Garcia, G. Lopez, Polyhedron 21 (2002) 1935.
[2] V.K. Jain, Transition Met. Chem. 18 (1993) 312–314.
[3] N. Manwani, R. Ratnani, R.N. Prasad, J.E. Drake, M.B. Hursthouse, M.E. Light, Inorg. Chem. Acta 351 (2003) 49–58.
[4] A.J. Burn, I. Gosney, C.P. Warrens, J.P. Wastle, J. Chem. Soc. Perkin Trans. 2 (1995) 265–268.
[5] M. Fuller, Z. Yin, M. Kasrai, G.M. Bancroft, E.S. Yamaguchi, P.R. Ryason, P.A. Willermet, K.H. Tan, Tribol. Int. 30 (1997) 305–315.
[6] H. So, Y.C. Lin, Wear 166 (1993) 17–26.
[7] S. Solak, C. Aydemir, M. Karakus, P. Lönnecke, Chem. Cent. J. 7 (2013) 89.
[8] V. Krishnakumar, R.J. Xavier, T. Chithambarathanu, Spectrochim. Acta Part A Mol. Biomol. Spectrosc. 62 (2005) 931–939.
[9] H. Chermette, Coord. Chem. Rev. 178–180 (1998) 699–721.
[10] C. Corminboeuf, F. Tran, J. Weber, J. Mol. Struct: THEOCHEM 672 (2006) 1–7.
[11] M. Karabacak, E. Sahin, M. Cinar, I. Erol, M. Kurt, J. Mol. Struct. 886 (2008) 148–157.
[12] X. Xuan, J. Wang, Y. Zhao, J. Zhu, J. Raman Spectrosc. 38 (2007) 865–872.
[13] M. Karabacak, A. Coruh, M. Kurt, J. Mol. Struct. 892 (2008) 125–131.
[14] N. Sundaraganesen, C. Meganathan, B.D. Joshua, P. Mani, A. Jayaprakash, Spectrochim. Acta Part A Mol. Biomol. Spectrosc. 71 (2008) 1134–1139.
[15] N. Sundaraganesen, C. Meganathan, B.D. Joshua, Spectrochim. Acta Part A Mol. Biomol. Spectrosc. 69 (2008) 871–879.
[16] X. Xuan, C. Zhai, Spectrochim. Acta A 79 (2011) 1663–1668.
[17] M.R. Anoop, P.S. Binil, S. Suma, M.R. Sudarsnakumar, et al., J. Mol. Struct. 969 (2010) 48–54.
[18] A. Atac, M. Karabacak, C. Karaca, E. Köse, Spectrochim. Acta A 85 (2012) 145–154.
[19] M. Karabacak, Z. Cinar, M. Kurt, S. Sudha, N. Sundaraganesan, Spectrochim. Acta A 85 (2012) 179–189.
[20] P.B. Nagabalasubramanian, M. Karabacak, S. Periandy, Spectrochim. Acta A 85 (2012) 43–52.
[21] M. Kurt, T.R. Sertbakan, M. Ozduran, M. Karabacak, J. Mol. Struct. 921 (2009) 178–187.
[22] Z. Cınar, M. Karabacak, M. Cınar, M. Kurt, P. Chinna babu, N. Sundaraganeman, Spectrochim. Acta A 116 (2013) 451–459.
[23] M. Karabacak, M. Cınar, M. Kurt, P. Chinna babu, N. Sundaraganeman, Spectrochim. Acta A 114 (2013) 509–519.
[24] N. Prabavathi, A. Nilufer, V. Krishnakumar, Spectrochim. Acta A 114 (2013) 449–474.
[25] N. Prabavathi, A. Nilufer, V. Krishnakumar, Spectrochim. Acta A 114 (2013) 101–113.
[26] M. Alcolea Palafox, V. Bena Jothy, Surabhi Singhal, I. Hubert Joe, Satendra Kumar, V.K. Rastogi, Spectrochim. Acta A 116 (2013) 509–517.
[27] L. Xiao-Hong, L. Tong-Wei, J. Wei-Wei, Y. Yong-Liang, Zhang Xian-Zhou, Spectrochim. Acta A 118 (2014) 503–509.
[28] I. Kara, H.H. Kart, N. Kolsuz, O.O. Karakus, H. Deligoz, Struct. Chem. 20 (2009) 113–119.
[29] Y. Li, H. Zhang, Y. Liu, F. Li, X. Liu, J. Mol. Struct. 997 (2011) 110–116.
[30] Y. Wang, Z. Yu, Y. Sun, Y. Wang, L. Lu, Spectrochim. Acta Part A Mol. Biomol. Spectrosc. 79 (2011) 1475–1482.
[31] S. Katsyuba, E. Vandyukova, Chem. Phys. Lett. 377 (2003) 658–662.
[32] J. Casanovas, A.M. Namba, S. Leon, G.L.B. Aquino, D.V.J. da Silva, C. Aleman, J. Org. Chem. 66 (2001) 3775–3782.
[33] N. Sundaraganesan, S. Ilakiamani, B. Anand, H. Saleem, B.D. Joshua, Spectrochim. Acta Part A Mol. Biomol. Spectrosc. 64 (2006) 586–594.
[34] J.B. Foresman, A.E Frisch, Exploring Chemistry with Electronic Structure Methods, Gaussian Inc., 1996.
[35] M.J. Frisch et al., Gaussian 09, Revision A.1, Gaussian Inc., Wallingford, CT, 2009.
[36] SQM version 1.0, Scaled Quantum Mechanical Force Field, Green Acres Road, Fayetteville, Arkansas, 2013. 72703.
[37] A.P. Scott, L. Radon, J. Phys. Chem. 100 (1996) 16502–16513.